Int. J. Heat Mass Transfer. Vol. 34, No. 4/5, pp. 1163–1174, 1991
Printed in Great Britain

0017–9310/91 $3.00 + 0.00

Experimental study of spray cooling with Freon-113

M. GHODBANE and J. P. HOLMAN
Civil and Mechanical Engineering Department, Southern Methodist University, Dallas, TX 75275-0335, U.S.A.

(*Received* 11 *July* 1989 *and in final form* 15 *June* 1990)

Abstract—Spray cooling heat transfer data for horizontal sprays on vertical constant heat flux surfaces with subcooled Freon-113 are presented. Using both full cone circular and square hydraulic spray nozzles, with three different orifice diameters, the flow rates are varied from 5.0 to 126.0 $cm^3\ s^{-1}$. The effects of mass flux, spray droplet velocity, droplet diameter, and distance between nozzle and heat source are investigated. Heat fluxes in excess of 60 $W\ cm^{-2}$ are achieved in the process. A non-dimensional generalized correlation for heat flux data applied to Freon-113 is successfully developed as

$$\frac{qx}{\mu_f h_{fg}} = 10.55(We)^{0.6}\left(\frac{c_f \Delta T}{h_{fg}}\right)^{1.46}.$$

The results of the study show that the Weber number defined as the ratio of inertial force to surface tension force has a large effect on the spray cooling process.

1. INTRODUCTION

BECAUSE of recent emphasis on removing high heat fluxes from electronic devices, spray cooling has become a subject of interest as an effective cooling technique. In spite of its importance, relatively little fundamental work has been done toward describing the physics of the heat transfer process involved in spray cooling.

The experiments described in this paper had as their objective surface cooling rates in excess of 60 $W\ cm^{-2}$ using subcooled Freon-113, with the heat source surface temperature maintained below 90°C. Much of the previous work in spray cooling has been concerned with surface temperatures well above the saturation temperature of the sprayed liquid; as a consequence, film boiling conditions were usually observed. Some of these conditions were studied by Hodgson and Sutherland [1].

Toda [2–4] reported extensive measurements of vertically downward sprayed water using a high pressure jet with a single hole nozzle directed at a horizontal surface. He classified the heat transfer process into three regions, according to the thermal behavior of the thin liquid film formed from mist drops on the heated surface. In this work a floating liquid film was always present on the surface during the film boiling stage. In contrast to Toda, Bonacina *et al.* [5, 6] performed experiments at low enough water flow rates to avoid the formation of a thin liquid film upon the heated surface, and thus experienced a spray evaporative cooling process. An investigation by Hoogendoorn and Den Hond [7] was concerned more with the Leidenfrost temperature of water sprays impinging on a hot surface than the overall heat transfer rates involved in cooling the surface.

A comprehensive discussion of the analytical and experimental evolution of spray cooling heat transfer was presented by Bolle and Moureau in their review essay [8]. Liu and Yao [9] introduced a model of spray cooling heat transfer based on distinguishing the different heat transfer mechanisms involved and interpreting the contribution of each mechanism to the overall heat transfer. The same procedure of heat transfer mechanisms was selected by Choi and Yao [10] in a study of normally impacting spray cooling. Despite the use of a spray generator which allowed an independent control over the spray parameters, they did not reveal new information, except that in a dense spray the droplet Weber number does not affect the heat transfer significantly.

Cho and co-workers [11, 12] conducted an experimental investigation on some characteristics of spray cooling and jet impingement methods. Using Freon-113 as a coolant, they correlated the burnout heat flux with the Weber number. They used the same approach to correlate spray cooling data as Katto and Monde [13]. According to their burnout heat flux data, heat transfer rates were greater with the spray method than the jet method.

The above studies were performed mostly at atmospheric pressure. A few experiments have been conducted under vacuum conditions. The effort of Grissom and Wierum [14] on spray cooling under vacuum conditions was to determine the temperature below which flooding would occur for a given spray striking a heated surface at a given pressure. The authors presented an analysis to predict the onset of flooding, but it applies only to normal atmospheric conditions because of a lack of spray droplet size diameter data at vacuum conditions. Kopchikov *et al.* [15] presented liquid film boiling heat transfer by

NOMENCLATURE

A	area of the test surface [m^2]
B	constant in equation (12)
c_f	liquid specific heat [kJ kg^{-1} C^{-1}]
D	constant in equation (13)
d_p	droplet diameter [μm]
d	nozzle orifice diameter [m]
g	gravitational accceleration [m s^{-2}]
h	heat transfer coefficient [W m^{-2} C^{-1}]
h_{fg}	enthalpy of vaporization [kJ kg^{-1}]
k	thermal conductivity [W m^{-1} C^{-1}]
L	characteristic length of the test surface [m]
m	exponent in equation (12)
$\dot{m}$	mass flux [kg s^{-1} m^{-2}]
N	spray concentration [drops m^{-3}]
$\dot{N}$	rate of production of droplets [drops s^{-1}]
P	ohmic dissipation from the test surface [W]
Pr	Prandtl number, $c_f\mu_f/k$ [dimensionless]
p	pressure [Pa]
Δp	pressure difference, $p_n - p_c$ [Pa]
q	heat flux [W m^{-2}]
q_{cond}	conduction heat flux [W m^{-2}]
q_{ohm}	ohmic dissipation flux [W m^{-2}]
q_r	radiation heat flux [W m^{-2}]
Re	Reynolds number, $\rho_f v d_p/\mu_f$ [dimensionless]
T	temperature [°C]
ΔT	temperature difference, $T_w - T_f$ [°C]
ΔT_{sub}	temperature difference, $T_s - T_f$ [°C]
V	volume flow rate [cm^3 s^{-1}]
v	droplet velocity [m s^{-1}]
We	Weber number, $\rho_f v^2 d_p/\sigma$ [dimensionless]
x	distance from nozzle to heat sources [cm].

Greek symbols

β	nozzle spray angle [deg]
γ	exponent in equation (13)
ε	emissivity [dimensionless]
μ	viscosity [kg m^{-1} s^{-1}]
σ	surface tension in equation (8) [dyn cm^{-1}]
σ	Stefan–Boltzmann constant (5.669×10^{-8} W m^{-2} K^{-4}) in equation (2).

Subscripts

c	chamber
f	evaluated at film conditions
f	liquid
n	nozzle
s	saturation conditions
sub	subcooled conditions
v	vapor
w	test surface
∞	environment.

spraying a heated surface with water and ethanol at pressures from 60 to 760 mm Hg. Despite the uncertainty in their data about the actual spray flow striking the surface, they still obtained a relationship for the heat transfer film coefficient. Yanosy [16] concluded in his investigation of water spray cooling in a vacuum that the reduction in heat transfer due to vacuum conditions was caused by the change in the thermal and transport properties of the water. He claimed the vacuum influenced the spray characteristics; thus, the heat transfer process was affected. However, he did not clearly state what properties were affected by the vacuum conditions.

Although the spray cooling method has various useful applications, the present study was motivated by the fact that an effective technique for cooling electronic equipment is needed to remove the high heat fluxes generated in densely packed electronic devices. For the most part, such devices must operate at temperatures below 80°C so the saturation temperature of the coolant must remain well below this value. Freon-113 is such a coolant, having a saturation temperature of 47.6°C at atmospheric pressure. The emphasis of this paper is primarily experimental and the objectives were to:

(1) Design and build a closed Freon-113 loop system with capabilities to vary droplet size, impact velocity, impact angle, heat flux, and surface temperature.

(2) Investigate the use of several commercial nozzles with different spray characteristics for effecting the spray cooling flow field.

(3) Collect a large amount of data to address the above issues.

(4) Make an extensive study of subcooled spray cooling and seek a generalized correlation of heat flux with the spray characteristics.

2. EXPERIMENTAL APPARATUS AND PROCEDURES

2.1. *Apparatus*

The experimental apparatus is shown in block diagram form in Fig. 1. All tubings were made of copper, valves and fittings were constructed of either brass or stainless steel, and Freon-113 was selected as the sprayed liquid because its properties are similar to those of dielectric liquids commonly used for direct immersion cooling of microelectronic components.

The closed loop spray system consisted of a supply tank, sight level gauge, heat exchanger, centrifugal pump, positive displacement flowmeter, and spray

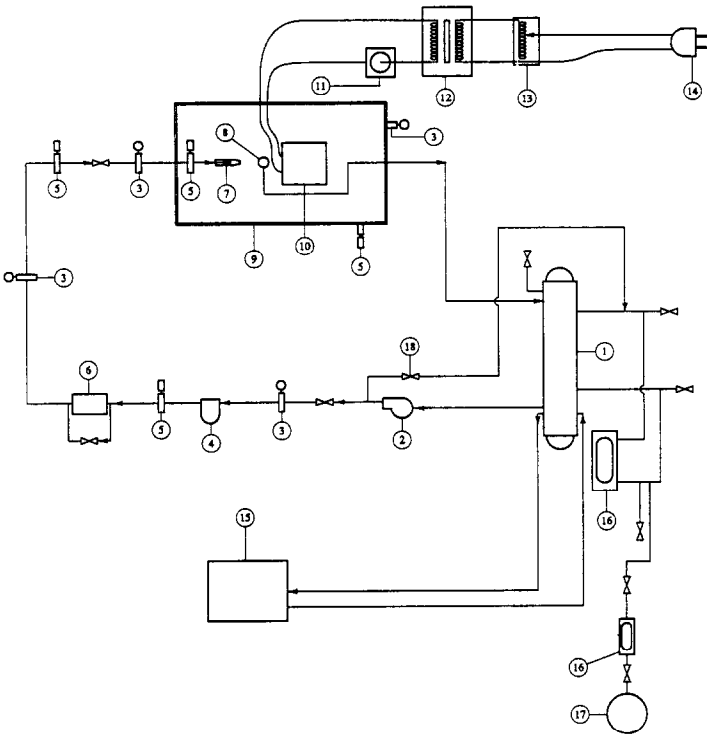

FIG. 1. Schematic layout of experimental apparatus: 1, heat exchanger; 2, pump; 3, pressure gauge; 4, filter; 5, pressure transducer; 6, flowmeter; 7, nozzle; 8, return drain; 9, test chamber; 10, test section; 11, current transformer; 12, voltage transformer; 13, variac; 14, a.c. power; 15, chiller; 16, sight gauge; 17, Freon supply tank; 18, valve (typical).

nozzle. An assortment of several commercial nozzles was available to vary the spray characteristics of the flow, spray distribution, and droplet sizes. These nozzles provided fairly uniform, full cone sprays. The shell and tube heat exchanger, in conjunction with the chiller, was used as a condensing unit for the returning vapor and hot liquid Freon from the test chamber.

The spraying process was initially performed in a 1 in. thick Plexiglas test chamber the dimensions of which were $91.44 \times 38.10 \times 38.10$ cm ($36 \times 15 \times 15$ in.). Later in the experiments the Plexiglas chamber was replaced by a similar stainless steel chamber to accommodate higher pressures created by rapid Freon evaporation. The latter chamber was equipped with two Plexiglas windows for visual and photographic observations. For both chambers two electrical cable connectors and two compression fittings for the thermocouples were attached through the bottom plate. Teflon inserts were used in swagelock fittings through which the thermocouples were introduced into the chambers.

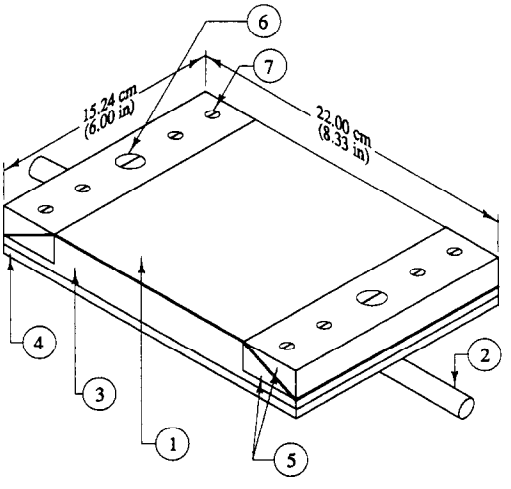

FIG. 2. Test section assembly: 1, stainless steel foil; 2, support shaft; 3, Teflon insulation; 4, support plate; 5, bus bar; 6, brass bolt; 7, flat head brass screw.

2.2. *Test surfaces*

The initial test section (15.24×15.24 cm) for the experiments is shown in Fig. 2. A smaller version (7.62×7.62 cm), using the same design was later built to study the effects of test surface size. The current carrying foil was a 0.0101 cm (0.004 in.) thick sheet of stainless steel 302 shim stock. As seen in the figure the left and right edges of the foil were free, while the front and back edges terminated in bus bars. Each bus bar was a two piece copper assembly with a clamp-like jaw that grasped the foil uniformly along all of its width. The foil was instrumented on its back face

through the insulating bed with thermocouples. In order to obtain local heat transfer readings, voltage taps were mounted on the bus bars for the large test section and directly on the foil for the small test section. Chromel–constantan, 0.00127 cm (0.0005 in.) thick cement-on foil thermocouples were used to minimize the disturbances of temperature measurements. The attachment of the thermocouples to the foil is accomplished by using a high temperature epoxy applied in minimal amounts.

Ten thermocouples were deployed at random on the back of the foil for the large test surface, while only five thermocouples were installed for the small test surface. To accommodate the bus bars, a recess was milled into the front face of the Teflon insulation, thus making the bus bars flush with the foil. For rigidity, an aluminum support plate backed up the Teflon insulation. This was done by means of nylon screws to avoid any electric contact between the heat source and the aluminum plate. One thermocouple was affixed to the backing plate for the purpose of evaluating possible heat losses across the insulating bed. Power was supplied to the foil from an a.c. source controlled by two variacs in series and a voltage transformer, as shown in Fig. 1.

A knowledge of the actual mass flux striking the test surface was desired. To measure the mass flux, a device was designed to collect the drops on the test section. Before or after each experimental run, the mass flux impinging on the surface was measured. The dimensions of the droplet catcher opening conforms exactly to the size of the sprayed test surface. After the collection procedure was accomplished, the measured mass flow rate divided by the area of the opening gave the mass flux. Table 1 indicates the results of a typical mass flux measurement. The results indicated a linear dependence of mass flux on distance from the nozzle to the test section opening. Although mass flux measurements were not made for all flow conditions, the linear dependence was believed to be reliable, and later served as a good correlating factor for the heat transfer data.

Particle size and droplet velocity were varied by altering the nozzle pressure. However, for nozzles, these last two mentioned parameters could not be varied independently since both are functions of pressure. To remedy this situation, an assortment of nozzles with different geometrical configurations was used to achieve several combinations of droplet sizes and velocities. The test section was always centered at the core of the spray for both circular and square cone spray nozzles in order to assure, as nearly as possible, a uniform cooling process.

Table 1. Variation of mass flux with striking distance for full cone spray nozzle ($d = 0.159$ cm)

Flow rate ($cm^3 s^{-1}$)	Ambient pressure range (kPa)	Heat source to nozzle distance (cm)	Mass flux ($kg s^{-1} cm^{-2}$)
126.18	45–101	18.42	8.381
		27.30	6.754
94.64	55–104	18.42	5.508
		27.30	3.434
76.97	62–104	18.42	4.118
		27.30	2.250
50.47	62–100	18.42	1.995
		27.30	1.180

While there were no direct measurements of impingement velocities, it was reasoned that the impingement velocities would be direct functions of the breakup velocities, which could then be used in correlation of the heat transfer data. This was indeed the case as will be shown in the data reduction section.

2.3. *Experimental procedure*

Before every experiment, the pump was operated at relatively high flow rates to completely purge the piping system of air. In addition, a vacuum pump was utilized to evacuate the remaining air from the chamber. The flow rate to the spray nozzle was controlled primarily by setting the bypass valve of the pump to obtain the desired supply pressure. The regulating and adjusting procedures took place through the throttling valve prior to the nozzle, while the bypass valve of the flowmeter was fully closed. Increasing the nozzle inlet pressure thereby increased the flow. The amount of Freon flowing through the nozzle was measured using a positive displacement flowmeter. The latter was provided with a bypass valve which was activated at the beginning of every experiment to prevent false readings and damage to the flowmeter. An indicator was connected to the flowmeter transmitter for direct reading of the flow rate through the spray nozzle.

A simple test with no spray was performed to check the reliability of the temperature and heat flux measurements. The total heat flux vs steady-state foil temperature was recorded under essentially free convection conditions. The measured heat input, minus the losses due to radiation and conduction represented the free convection transfer from the test surface. The free convection data were obtained by fixing the power input to the test surface for as much as 3 h and noting the corresponding steady-state temperature. The calculated values are about 30% above conventional free convection correlations, but forced convection currents in the room could easily account for this increase. This relatively severe test indicates that the temperature and heat flux measurements were reliable.

The exposed surface area was carefully measured before each test section assembly. The surface was left in the original highly polished condition and periodically cleaned with acetone and alcohol. The surface temperature of the test section was varied by increasing the voltage input to the test surface by means of a step-down transformer. All the experimental runs

progressed from low power to high power. The amount of heat was determined by measuring the voltage drop across the hot plate with a digital voltmeter. The current in the circuit was measured by a current transformer in combination with a standard resistor and digital voltmeter. The average temperature of the foil was measured by thermocouples attached to its back. The thermocouple readings were recorded by a data logger, which was connected to a computer for data storage and reduction on disks. Pressures and temperatures at different points of the experimental loop were accurately monitored to ensure that steady-state conditions were maintained during each experimental run.

3. EXPERIMENTAL RESULTS AND DISCUSSION

3.1. *General description*

To describe spray cooling heat transfer using hydraulic nozzles, it would be desirable to have information on droplet size distribution, impact velocity, coolant mass flux, quantity of liquid evaporated, and heat flux minus the losses needed to accomplish the evaporation process. It was not possible to measure all of these variables with the apparatus, but consistent calculation procedures were adopted so that the various data could be manipulated toward a correlation for the heat transfer behavior.

The liquid supplied to the nozzles was usually in a subcooled state; the temperature ranged from 5 to 10°C. In such cases the first heat transfer process encountered was that of forced convective heat transfer in a single phase flow, where the bulk liquid temperature was generally less than the saturation temperature value (47°C at 1 atm). Boiling was stipulated at the point in each experimental run when the test surface temperature exceeded the liquid saturation temperature based on chamber pressure. The process up to the point at which the bulk liquid temperature reached the saturation temperature was defined as subcooled boiling.

A series of experiments were performed on spray cooling in which relationships between the heat transfer rate and the spraying conditions were examined. A typical data point consisted of a value of heat flux supplied to the test surface, the corresponding average surface temperature taken as an arithmetic average of the individual surface temperatures, the liquid temperature, nozzle pressure, ambient temperature, and chamber pressure. A minimum of eight data points made up a run, starting at low power and ending at high power. Sometimes, the burnout point, which resulted in the destruction of the test surface, could not be predicted in advance. However, in some cases a fog-like condition in the chamber gave a signal that the burnout point of the run was being reached.

A number of parameters was varied. All the runs involved variation of spray flow rate, heat source to nozzle distance, drop size, and impact velocity. A summary of experimental parameters such as distance from the nozzle to the test object, nozzle orifice diameter, and droplet breakup velocity are given in Table 2.

Table 2. Summary of experimental data

Nozzle orifice diameter (cm)	Heat source to nozzle distance (cm)	Droplet velocity ($m\ s^{-1}$)
(a) Large test surface		
0.238 square full cone	18.42	13.70
		10.25
		8.40
		5.40
	27.30	13.70
		10.25
		8.40
		5.40
	34.92	13.70
		10.25
		8.40
		5.40
0.159 circular full cone	18.42	27.30
		19.10
	27.30	21.50
	34.92	25.45
(b) Small test surface		
0.159 circular full cone	18.42	27.30
		19.10
		15.60
		9.10
	27.30	27.30
		19.10
		15.60
		9.10
0.063 circular full cone	18.42	28.50
		28.50
		10.84

3.2. *Experimental data reduction*

The experimental data were reduced with a computer program which translates the measured quantities such as nozzle pressure, chamber pressure, surface temperature, mass flow rate, and voltage across the foil, heat flux, droplet diameter, impact velocity and mass flux into the important heat transfer parameters. The equations and methods used to compute the above quantities are described in the following sections.

3.2.1. *Heat flux and surface temperature.* The numerical values of the local heat flux q were obtained from

$$q = q_{\text{ohm}} - q_{\text{cond}} - q_{\text{r}} \tag{1}$$

$$q = \frac{P}{A} - \frac{(T_{\text{w}} - T_{\text{b}})}{R_{\text{b}}} - \varepsilon\sigma(T_{\text{w}}^4 - T_{\infty}^4) \tag{2}$$

where P is the ohmic dissipation from the test surface. Calculations showed the radiation term to be negligible.

Since temperature measurements in the test section were made on the back of the foil which is at a distance

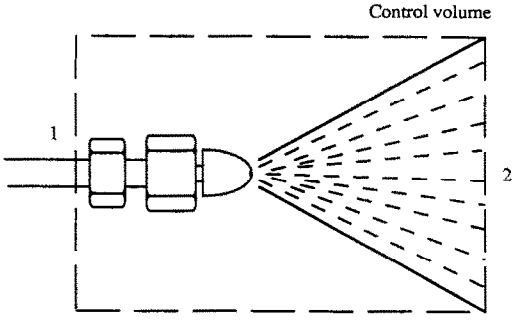

FIG. 3. Control volume for energy balance.

of 0.1016 mm from the sprayed surface, corrections to surface temperature values were required. A simple one-dimensional correction was adequate for determining the surface temperature. The error involved in this case was small and was further reduced when the average temperature was computed.

The uniformity of the surface temperature distribution was indicative of the overall uniformity cooling of the surface, $T_w(\max) - T_w(\min)$ was not always consistent, but did not exceed 5°C. Usually, $T_w(\min)$ occurred in the vicinity of the center of the test surface, while $T_w(\max)$ was often the temperature at one of the four corners or along the clamped edges of the foil. Thus the surface temperature for heat transfer calculations was taken as the arithmetic average of the thermocouple readings

$$T_w = \sum_{i=1}^{n} \frac{T_w(i)}{n} \tag{3}$$

when $n = 10$ for the large test surface and $n = 5$ for the small test surface.

3.2.2. *Droplet velocity.* It was not possible to measure the velocity of drops in this experiment. An attempt was made using a video system in combination with a stroboscope, but only a qualitative observation was obtained. The droplet impact velocity was believed to be one of the important physical parameters influencing heat transfer in spray cooling and was taken to be a direct function of breakup velocity, which was determined by the following approximate analysis.

The breakup velocity of the droplets was estimated using a simple control volume energy balance around the nozzle with the following assumptions:

(a) Losses are negligible, i.e. no droplets leaving the control volume through the sides.

(b) Gravity forces are negligible.

(c) Air and vapor circulation inside the spray are negligible.

(d) The pressure inside the spray is assumed to be uniform and equal to the ambient pressure.

As shown in Fig. 3, upstream from the nozzle the Freon has a velocity v_1, pressure p_1 and flows through a tube of area A_1. Downstream, the spray consists of droplets of diameter d_p and velocity v_2 at pressure p_2. The energy balance is given by

$$\rho_1 v_1 A_1 \left(\frac{v_1^2}{2} + \frac{p_1}{\rho_1}\right) = \dot{N}\frac{\rho_2 \pi d_p^3}{6}\left(\frac{v_2^2}{2} + \frac{p_2}{\rho_2}\right) + \dot{N}\sigma\pi d_p^2 \tag{4}$$

where $\dot{N}$ is the rate of production of droplets and σ the surface tension. Assuming constant liquid density ($\rho_1 = \rho_2$) the continuity equation gives

$$\rho_1 v_1 A_1 = \dot{N}\rho\pi\frac{d_p^3}{6} \tag{5}$$

then

$$\dot{N} = \frac{6 v_1 A_1}{\pi d_p^3}. \tag{6}$$

This assumes the droplets are uniform in size. Substituting equation (6) into equation (4) and solving for v_2 which represents the droplet breakup velocity gives the following equation:

$$v_2 = \left(v_1^2 + \frac{2\Delta p}{\rho} - \frac{12\sigma}{\rho d_p}\right)^{1/2} \tag{7}$$

where σ the surface tension and d_p the droplet diameter are obtained from equations (8) and (9), respectively. The notation v_2 for the droplet breakup velocity is used only for the control volume analysis. Throughout the study the droplet breakup velocity is always denoted by v. Values for the surface tension of the Freon were calculated from the following relationship given in the Dupont Technical Bulletin [17]:

$$\sigma = 3.14749(\rho_\ell - \rho_v)^4 \tag{8}$$

where vapor and liquid densities are evaluated at the desired temperature. The units used in equation (8) are dyn cm^{-1} for the surface tension and g cm^{-3} for the densities.

3.2.3. *Droplet diameter.* Droplet sizes varied over a relatively wide sprectrum from 210 to 980 μm, controlled by the nozzle type, size, and spraying pressure. The most commonly used parameter to describe spray droplet size is the volume median diameter or the mass median diameter. Mugele and Evans [18] and Dombrowski and Munday [19] specified other common means and their applications. By definition, the mass median diameter represents 50% of the total mass sprayed consisting of drops with a diameter larger than the mass median diameter and 50% of the total mass sprayed consisting of drops with a diameter smaller than the mass median diameter.

After careful analysis of correlations proposed by Rothe and Block [20], Toda [3], Bonacina *et al.* [6] and Simmons and Harding's work [21, 22], it was determined that the most reliable correlation, and the one in best agreement with the nozzle manufacturer's specifications, was the empirical correlation of mass median diameter given in Bonacina *et al.*'s work

$$d_p = \frac{9.5d}{\left(\Delta p^{0.37} \sin \frac{\beta}{2}\right)} \quad (9)$$

in which Δp, d and β represent the differential pressure between the nozzle pressure and the chamber pressure in Pascals, the nozzle orifice diameter, and the nozzle spray angle, respectively.

Properties of the working fluid, except for latent heat h_{fg} which was computed at the saturation temperature corresponding to the chamber pressure, were evaluated at the film temperature which represented the average of the local surface and spray temperature

$$T_f = \frac{T_w + T_\ell}{2}. \quad (10)$$

The thermodynamic properties as functions of temperature and pressure were obtained from the American Society of Heating, Refrigerating, and Air Conditioning Engineers [23] and Dupont Technical Bulletins [17, 24].

3.3. *Data correlation and discussion*

Data were obtained for various combinations of parameters such as flow rate, droplet size, test surface area, striking distance, and droplet breakup velocity. Table 3 presents a summary of the range of variables covered during the course of the experiments. The experimental results using the large test surface (15.24×15.24 cm) are depicted in Fig. 4 showing the overall heat transfer as a function of the temperature difference ($T_w - T_\ell$), at various liquid flow rates for fixed heat source to nozzle distances.

The heat transfer in these experiments was mainly subcooled boiling which is usually a combination of convective and boiling heat transfer. This heat transfer depends on $T_w - T_\ell$ instead of $T_w - T_s$.

The cooling curves indicate that the heat transfer capability increased as the flow rate was increased. Increasing the flow rate also delayed the onset of saturated nucleate boiling and retarded burnout. Figure 5 shows similar cooling curves for the small test surface. For both surfaces, the heat flux curves maintained a positive gradient up to a temperature of 90°C. As $T_w - T_\ell$ increased, the slope of the cooling curves steepened and the data began to fall on the saturated nucleate boiling curves. This indicates that $T_w - T_\ell$ is an effective driving force in the subcooled spraying process.

Table 3. Range of test variables

Variable	Range
Test surface area	15.24×15.24 cm and 7.62×7.62 cm
Liquid flow rate	5–126.0 cm^3 s^{-1}
Heat source to nozzle distance	18.0–35.0 cm
Breakup droplet velocity from equation (7)	5.40–28.0 m s^{-1}
Droplet diameter from equation (9)	210–980 μm
Surface temperature	20–90°C
Spray temperature	5–10°C
Heat flux	0.12–50.0 W cm^{-2}
Weber number, *We*	2200–13 750
Reynolds number, *Re*	2557–61 878
Prandtl number, *Pr*	7.5–10.5

Since the droplet velocity and diameter were determined from the liquid flow rate, it is logical to conclude that the droplet velocity and its diameter influence the overall spray cooling effectiveness. Nozzle to heat source distance was found to have a major effect on the spray cooling. Figure 6 displays the heat flux vs $(T_w - T_\ell)$ for a fixed flow rate at varying nozzle to heat source distance. The figure shows that the spray cooling is more effective at shorter distances. As was shown in Table 1 the mass flux decreases with increasing striking distance, in a linear way. It would be expected, then, that the heat transfer would follow a similar variation, and this turns out to be the case.

Before describing the approach taken to correlate the data, some qualitative observations may be mentioned.

(a) Even at the burnout state, which is reached when the test piece starts glowing red the amount of vapor observed in the chamber was negligible compared to the amount of liquid. This effect was immediately followed by a violent vapor generation in the test chamber indicating the destruction of the test surface.

(b) The number of droplets bouncing back from the walls of the chamber onto the heated surface was small.

The conduction losses through the insulation bed and the radiation losses from the test surface were negligible.

Figures 4 and 5 clearly show that the heat flux curves follow a similar variation with $T_w - T_\ell$. Consequently, the primary variable controlling the heat transfer mechanism is the temperature difference $T_w - T_\ell$.

In developing a semi-empirical formulation for the heat flux in spray cooling, one would expect a dependency of the heat flux on Weber number. It characterizes the impacting dynamics of the droplets since it is a ratio of inertial force to surface tension force. The high Weber number in the present study impeded the formation of a vapor blanket between the heated surface and the droplets. The velocity used in computing the Weber number is the spray breakup velocity given by equation (7), because we assume the impingement velocity is strongly related to breakup velocity.

Because of local agitation of the fluid at the heated surface, one might anticipate that the droplet Reynolds number would appear in the correlation. The effect may alternately be described using the Weber number in combination with the liquid viscosity in the correlation equation.

The heat flux curves depicted in Figs. 4 and 5 show

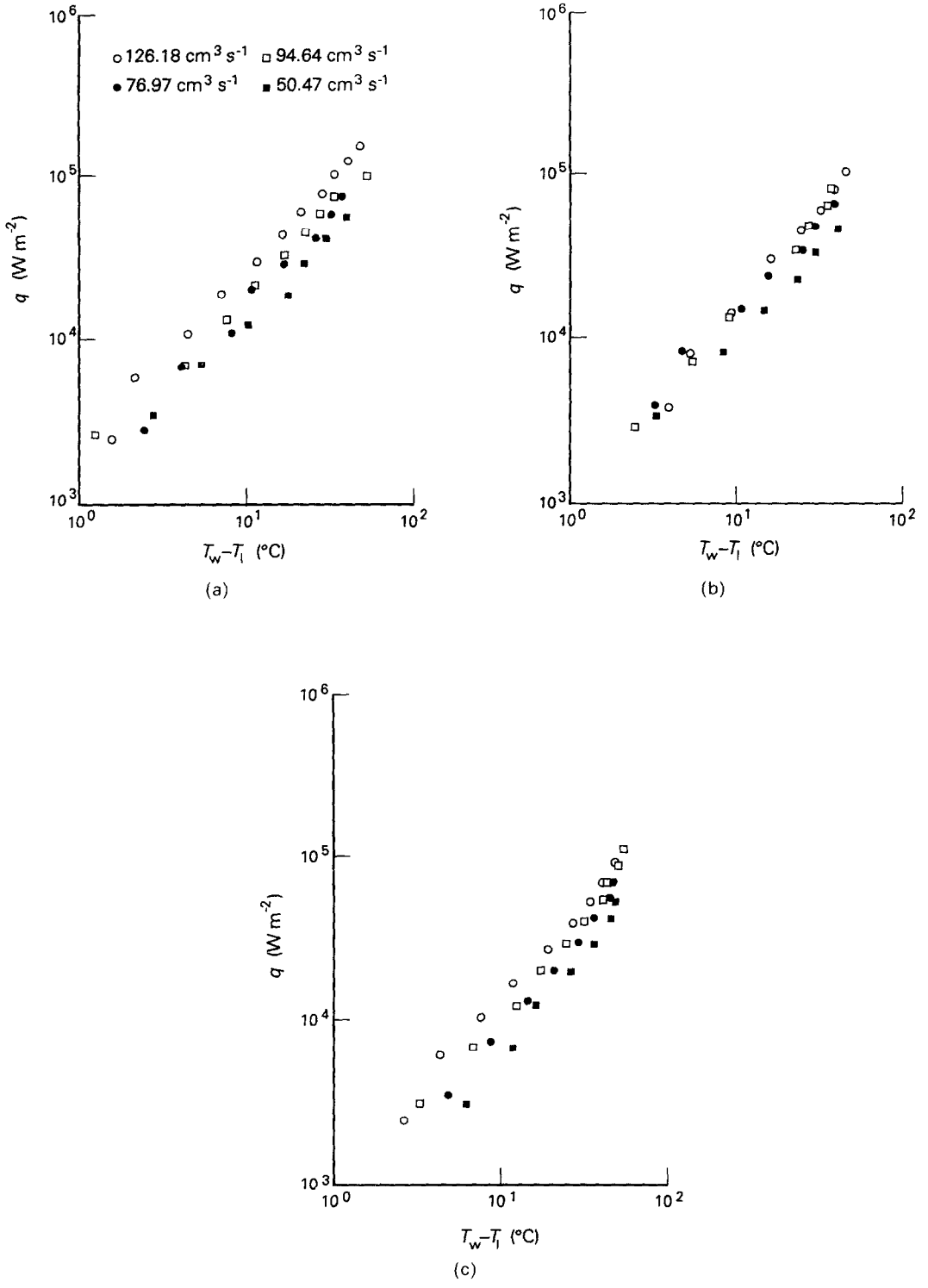

FIG. 4. Spray cooling data of large test surface (15.24 × 15.24 cm) using full cone square spray nozzle ($d = 0.238$ cm): (a) $x = 18.42$ cm; (b) $x = 27.30$ cm; (c) $x = 34.92$ cm.

that the heat source size does not affect the overall heat transfer behavior, as long as the heat source is kept within the core of the spray. This indicates that the sprays used in the experiments were quite uniform.

According to Table 1, the heat source to nozzle distance is definitely a mass flux parameter, and behaves nearly in a linear manner. Therefore, the mass flux may be expressed in terms of heat source to nozzle

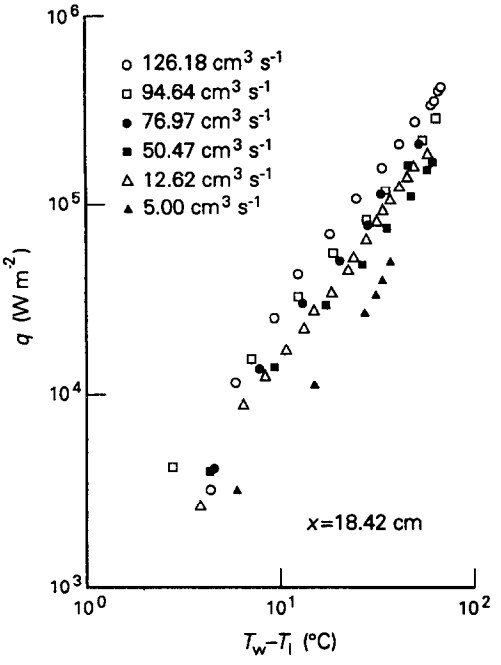

FIG. 5. Spray cooling data of small test surface (7.62 × 7.62 cm) using two different full cone spray nozzles: $d = 0.159$ cm for 126.18–50.47 cm^3 s^{-1}; $d = 0.08$ cm for 12.62 and 5.00 cm^3 s^{-1}).

distance for purposes of correlating the data. The effects of heat source to nozzle distance on spray cooling are shown in Fig. 6. Based upon the preceding concepts and the experimental data, a functional expression for the spray cooling heat flux was assumed as

$$q = f(\Delta T, We, \mu_l, x). \tag{11}$$

A cross plot of $(q/c_l\Delta T)$ vs Weber number for every x position showed the slope of the line on a log–log plot to be approximately 0.6 for both test surfaces. To show the effect of the heat source to nozzle distance, plots of $(qx/We^{0.6})$ vs $(T_w - T_l)$ were generated as shown in Fig. 7. This type of plot reflects the approximately inverse variation of mass flux of droplets with x. On the basis of these plots the data were correlated by an equation of the form

$$\frac{qx}{We^{0.6}} = B(\Delta T)^m \tag{12}$$

where the values of B and m could be determined by superimposing a correlation line on the plot.

While equation (12) provides useful information on Freon-113 spray cooling, it is helpful to consolidate the wide range of data by producing a non-dimensional general correlation. Therefore, fluid properties, such as liquid specific heat and latent heat were incorporated into the correlation. Then, equation (12) may be written in non-dimensional form as

$$\frac{qx}{\mu_l h_{fg}} = D(We)^{0.6}\left(\frac{c_l\Delta T}{h_{fg}}\right)^y. \tag{13}$$

Plots such as Figs. 8 and 9 were obtained showing that the experimental data seem to be correlated quite adequately by equations of the form of equation (13).

It should be noted that the scatter of the data for

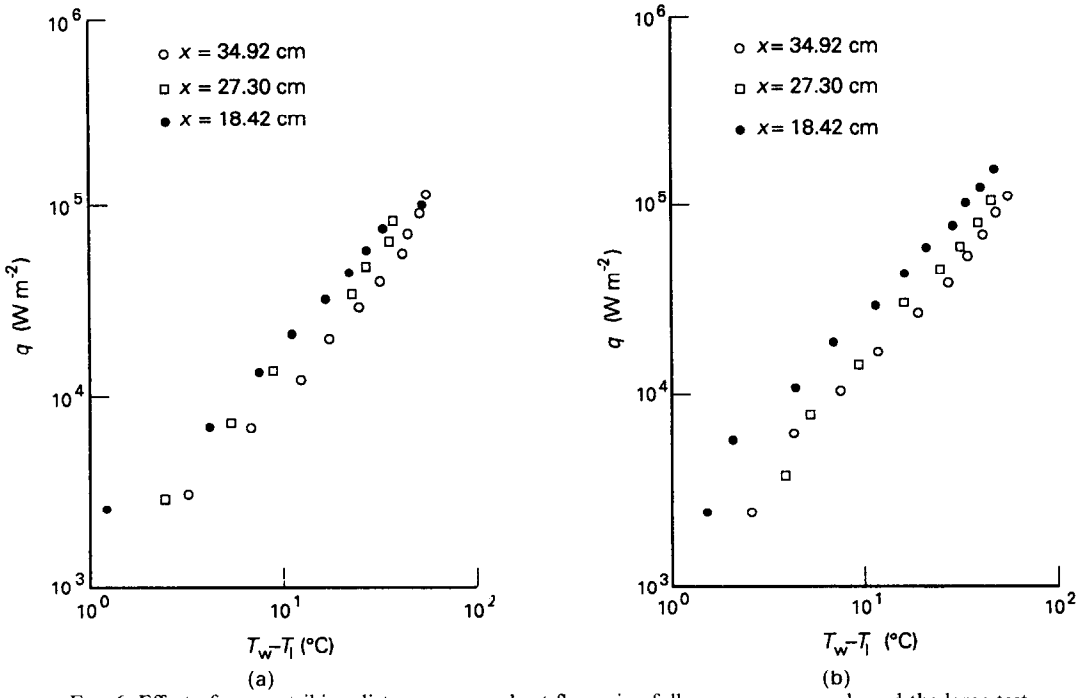

FIG. 6. Effect of spray striking distance x upon heat flux using full cone square nozzle and the large test surface: (a) $V = 94.64$ cm^3 s^{-1}; (b) $V = 126.18$ cm^3 s^{-1}.

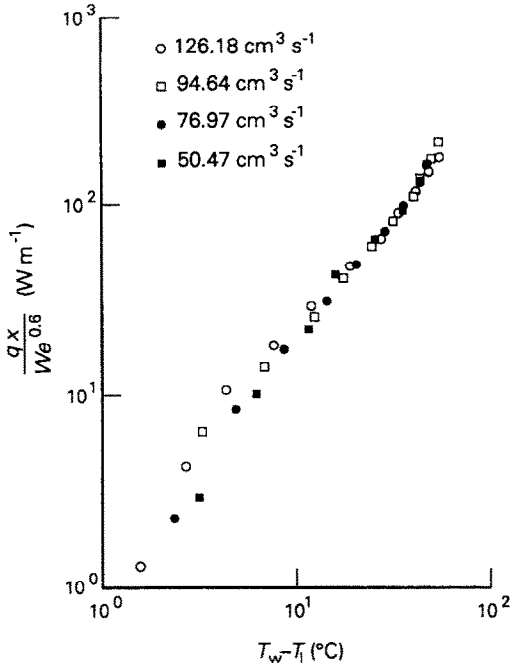

FIG. 7. Correlation of spray cooling heat transfer data using full cone square spray nozzle ($d = 0.238$ cm) and the large test surface.

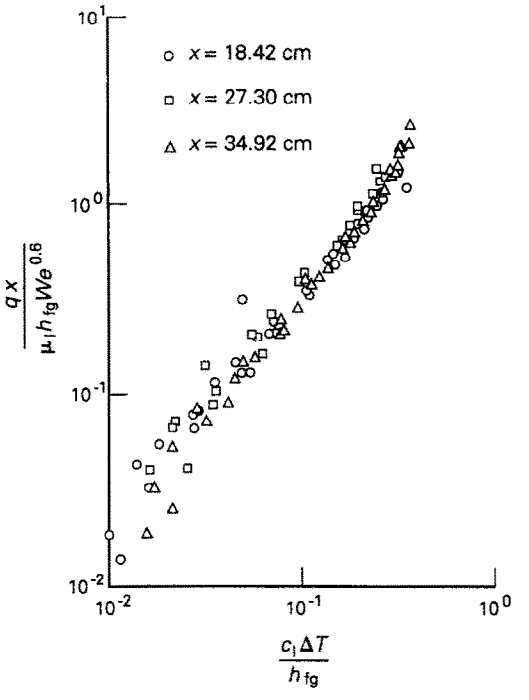

FIG. 8. Non-dimensional correlation of spray cooling data using full cone square spray nozzle ($d = 0.238$ cm) and the large test surface (each x position represents four flow rates).

lower values of the temperature difference $(T_w - T_f)$ results mainly from the experimental uncertainty in the measurement of the temperatures. Relatively small uncertainties in T_w and T_f magnify the uncertainty in ΔT when ΔT is small.

To arrive at a generalized correlation, the exponent γ in equation (13) can be determined by superimposing Figs. 8 and 9 into a single plot shown in Fig. 10. The constant D in equation (13) can be determined from the solid straight lines in Fig. 10. As a result, the spray cooling heat flux with subcooled Freon-113 is correlated by

$$\frac{qx}{u_f h_{fg}} = 10.55(We)^{0.6}\left(\frac{c_f \Delta T}{h_{fg}}\right)^{1.46}. \qquad (14)$$

It should be noted that the liquid subcooling term $c_f(T_s - T_f)/h_{fg}$ was kept at nearly a constant value of 0.22.

4. CONCLUSIONS

The present study was directed toward cooling flush-mounted vertical heat sources with horizontal sprays, which simulate electronic devices. The work provided meaningful insight into various mechanisms of impacting spray heat transfer. It also provided quantitative information on subcooled convection boiling heat transfer. With the experimental data gathered and the visual observations made in this investigation, it is possible to draw the following conclusions.

(1) Experimental data of spray cooling indicate that the heat transfer characteristics are independent of the heat source surface area as long as the spray is uniform. Commercial nozzles may be used to generate satisfactorily uniform sprays. Three nozzle orifice

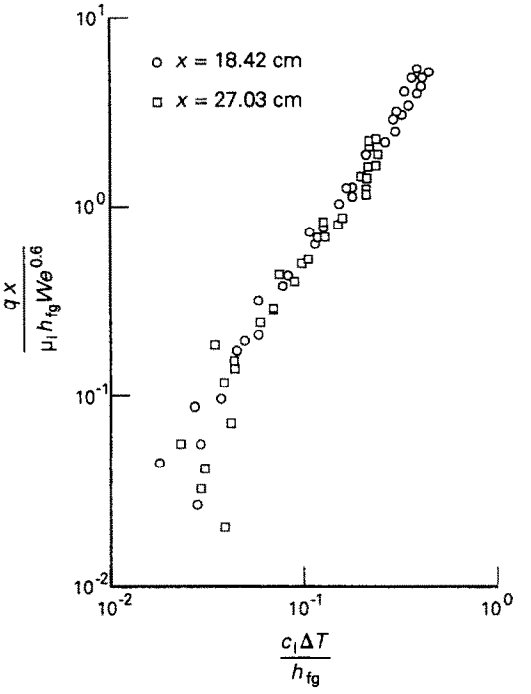

FIG. 9. Non-dimensional correlation of spray cooling data using full cone spray nozzle ($d = 0.159$ cm) and the small test surface (each x position represents four flow rates).

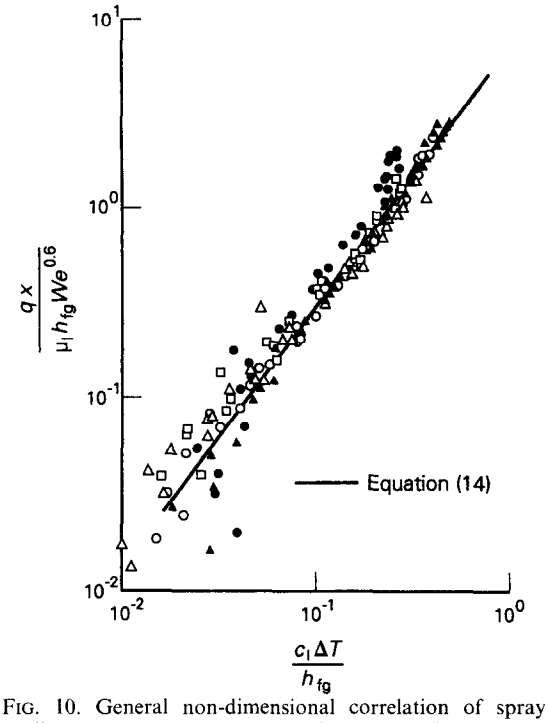

FIG. 10. General non-dimensional correlation of spray cooling heat transfer (open symbols represent data of large test surface while full symbols represent data of small test surface).

diameters, and two full-cone spray configurations were used in this investigation.

(2) The heat transfer of impacting spray increases with the increasing droplet mass flux in an approximately linear fashion.

(3) A high degree of liquid subcooling ($\Delta T_{sub} = 30°C$) delays the onset of saturated nucleate boiling of the spray and subsequent burnout.

(4) The Weber number has a strong effect on the overall heat transfer characteristics of liquid spray cooling.

(5) Dissipation of heat fluxes up to 50 W cm^{-2} from electronic devices can be accommodated by subcooled Freon-113 spray cooling, with the surface temperature below 80°C.

(6) Finally, a general correlation equation has been developed for subcooled Freon-113 spray cooling heat transfer over a wide range of test conditions and parameters. The non-dimensional correlation of the present spray cooling heat transfer is of the form

$$\frac{qx}{u_f h_{fg}} = 10.55(We)^{0.6}\left(\frac{c_f \Delta T}{h_{fg}}\right)^{1.46}.$$

Ranges of the various physical parameters are shown in Table 3.

Acknowledgements—The authors gratefully acknowledge sponsorship of this work by the Strategic Defense Initiative and the Aero Propulsion and Power Laboratory, Wright Research and Development Center, under contract No. F33615-86-C-2704.

REFERENCES

1. J. W. Hodgson and J. E. Sutherland, Heat transfer from a spray cooled isothermal cylinder, *Ind. Engng Chem. Fundam.* **7**, 567–571 (1968).
2. S. Toda and H. Uchida, A study of mist drops on a heated surface at high temperatures and high heat fluxes, *Proc. Fourth Int. Heat Transfer Conf.*, Paris–Versailles, Vol. 5, p. B5.3 (1970).
3. S. Toda, A study of mist cooling, *Heat Transfer—Jap. Res.* **2**, 39–50 (1972).
4. S. Toda, A study of mist cooling: theory of mist cooling and its fundamental experiments, *Heat Transfer—Jap. Res.* **3**, 1–44 (1974).
5. C. S. Bonacina, Del Guidice and G. Comini, Evaporization of automized liquids on hot surface, *Lett. Heat Mass Transfer* **2**, 401–406 (1975).
6. C. S. Bonacina, Del Guidice and G. Comini, Dropwise evaporization, *J. Heat Transfer* **101**, 441–446 (1979).
7. C. J. Hoogendoorn and R. Den Hond, Leidenfrost temperature and heat transfer coefficients for water sprays impinging on a hot surface, *Proc. Fifth Int. Heat Transfer Conf.*, Tokyo, Vol. 4, pp. 135–138 (1974).
8. L. Bolle and J. C. Moureau, Spray cooling of hot surfaces. In *Multiphase Science and Technology*, pp. 1–97. Hemisphere, Washington, DC (1977).
9. L. Liu and S. C. Yao, Heat transfer analysis of droplet flow impinging on a hot surface, *Proc. 7th Int. Heat Transfer Conf.*, Munich, Vol. 4, pp. 161–166 (1982).
10. K. Choi and S. C. Yao, Mechanisms of film boiling heat transfer of normally impacting spray, *Int. J. Heat Mass Transfer* **30**, 311–318 (1987).
11. C. S. K. Cho and J. Sharma, Burnout in a high heat flux element with subcooled freon. In *Temperature/Fluid Measurements in Electronic Equipment*, ASME HTD-Vol. 89, pp. 37–43. Boston (1987).
12. C. S. K. Cho and K. Wu, Comparison of burnout characteristics in jet impingement cooling and spray cooling, *Natn. Heat Transfer Conf. Proc.*, Houston, ASME HTD-Vol. 96, pp. 561–567 (1988).
13. Y. Katto and M. Monde, Study of mechanism of burnout in high heat flux boiling system with an impinging jet, *Proc. Fifth Int. Heat Transfer Conf.*, Tokyo, p. B6.2 (1974).
14. W. Grissom and F. A. Wierum, Liquid spray cooling of a heated surface, *Int. J. Heat Mass Transfer* **24**, 261–271 (1981).
15. I. A. Kopchikov, G. I. Voronin, T. A. Kolach, D. A. Labuntsov and P. D. Lebedev, Liquid boiling in a thin film, *Int. J. Heat Mass Transfer* **12**, 791–796 (1969).
16. J. L. Yanosy, Water spray cooling in a vacuum, Ph.D. Dissertation, University of Connecticut, Storrs, Connecticut (1985).
17. Surface tension of the Freon compounds, Dupont Technical Bulletin D-27, Wilmington, Delaware (1967).
18. R. A. Mugele and H. D. Evans, Droplet size distribution in sprays, *Ind. Engng Chem.* **43**, 1317–1324 (1951).
19. N. Dombrowski and G. Munday, Spray drying, *Biochem. Biol. Engng Sci.* **2**, 209–218 (1972).
20. P. H. Rothe and J. A. Block, Aerodynamic behavior of liquid sprays, *Int. J. Multiphase Flow* **3**, 263–272 (1977).
21. H. C. Simmons, Prediction of sauter mean diameter for gas turbine fuel nozzles of different types, *J. Engng Pwr* **102**, 646–652 (1980).
22. H. C. Simmons and C. F. Harding, Some effects of using water as a test fluid in fuel nozzle spray analysis, *J. Engng Pwr* **103**, 118–123 (1981).
23. R. B. Stewart, R. T. Jacobson and S. G. Penoncello, *Thermodynamics Properties of Refrigerants*, ASHRAE S. I. Edition. Atlanta, Georgia (1988).
24. Transport properties of fluorocarbons, Dupont Technical Bulletin C-30, Wilmington, Delaware (1973).

ETUDE EXPERIMENTALE DU REFROIDISSEMENT PAR PULVERISATION DE FREON-113

Résumé—On présente des expériences de refroidissement par pulvérisation horizontale de Freon-113 sous-refroidi sur des surfaces verticales chauffées à flux uniforme. En utilisant des orifices circulaires coniques ou droits avec différents diamètres, les débits varient entre 5,0 et 126,0 $cm^3\ s^{-1}$. On étudie les effets du flux de masse, de la vitesse des gouttes pulvérisées, du diamètre des gouttes et de la distance entre l'orifice et la surface. On atteint des densités de flux supérieurs à 60 W cm^{-2}. Une formule sans dimension pour le Freon-113 est développé avec succès:

$$\frac{qx}{\mu_l h_{fg}} = 10{,}55(We)^{0.6}\left(\frac{c_l \Delta T}{h_{fg}}\right)^{1.46}.$$

Les résultats montrent que le nombre de Weber défini comme le rapport de la force d'inertie à la tension interfaciale a un large effet sur le mécanisme de refroidissement par pulvérisation.

EXPERIMENTELLE UNTERSUCHUNG DER SPRÜHKÜHLUNG MIT R-113

Zusammenfassung—Es werden Wärmeübergangskoeffizienten für die Sprühkühlung horizontaler Sprühnebel aus unterkühltem R-113 an senkrechten Flächen mit konstanter Wärmestromdichte vorgestellt. Es werden sowohl Sprühdüsen mit vollem Kreiskonus als auch Quadratkonus verwendet. Bei drei verschiedenen Blendendurchmessern wird der Volumenstrom von 5–126 $cm^3\ s^{-1}$ variiert. Der Einfluß der Massenstromdichte, der Tropfengeschwindigkeit, des Tropfendurchmessers und des Abstandes zwischen Düse und Wärmequelle wird untersucht. Dabei übersteigt die Wärmestromdichte 60 W cm^{-2}. Für die Wärmestromdichte bei Verwendung von R-113 wird folgende dimensionslose verallgemeinerte Korrelation entwickelt:

$$\frac{qx}{\mu_l h_{fg}} = 10{,}55(We)^{0.6}\left(\frac{c_l \Delta T}{h_{fg}}\right)^{1.46}.$$

Die Ergebnisse zeigen, daß die Weber-Zahl (Verhältnis aus Trägheitskraft und Oberflächenkraft) einen großen Einfluß auf die Sprühkühlung ausübt.

ЭКСПЕРИМЕНТАЛЬНОЕ ИССЛЕДОВАНИЕ РАСПЫЛИТЕЛЬНОГО ОХЛАЖДЕНИЯ С ИСПОЛЬЗОВАНИЕМ ФРЕОНА-113

Аннотация—Приводятся данные по теплопереносу при распылительном охлаждении между горизонтальными струями переохлажденного фреона-113 и вертикальными поверхностями с постоянным тепловым потоком с тремя различными диаметрами отверстий расходы изменялись от 5,0 до 126,0 $см^3\ с^{-1}$. В зависимости от применения круглого, конического или квадратного гидравлического распылительных сопел исследуются эффекты массового потока, скорости капель распыла, диаметра капель и расстояния между соплом и источником тепла. В рассматриваемом процессе достигнуты значения теплового потока свыше 60 Вт $см^{-2}$. Удалось получить безразмерное обобщенное соотношение для данных по тепловому потоку применительно к фреону-113

$$\frac{qx}{\mu_l h_{fg}} = 10{,}55(We)^{0.6}\left(\frac{c_l \Delta T}{h_{fg}}\right)^{1.46}.$$

Результаты исследования показывают, что число Вебера, определяемое как отношение силы инерции к силе поверхностного натяжения, оказывает значительное влияние на процесс охлаждения распыла.